Langmuir

Article

pubs.acs.org/Langmuir

Hybrid Polyion Complex Micelles Formed from Double Hydrophilic Block Copolymers and Multivalent Metal Ions: Size Control and Nanostructure

Nicolas Sanson,[†,∥] Frédéric Bouyer,[†] Mathias Destarac,[‡,⊥] Martin In,[§] and Corine Gérardin*[,†]

[†]Institut Charles Gerhardt, UMR 5253 CNRS/ENSCM/UM2/UM1, 8 Rue de L'Ecole Normale, 34296 Montpellier Cedex 5, France

[‡]Centre de Recherches et Technologies d'Aubervilliers, Rhodia Opérations, 52 Rue de la Haie Coq, 93308 Aubervilliers Cedex, France

[§]Laboratoire Charles Coulomb, UMR 5221 CNRS/UM2, Place Eugène Bataillon, 34095 Montpellier Cedex 5, France

[∥]Laboratoire de Physicochimie des Polymères et Milieux Dispersés—Sciences et Ingénierie de la Matière Molle, UMR7615, UPMC Sorbonne Universités, ESPCI ParisTech, CNRS, Ecole Supérieure de Physique et de Chimie Industrielles, 10 Rue Vauquelin, 75231 Paris Cedex 5, France

[⊥]Université de Toulouse, UPS, LHFA, 118 Route de Narbonne, 31062 Toulouse, France and CNRS, LHFA, UMR 5069, 31062 Toulouse, France

Supporting Information

ABSTRACT: Hybrid polyion complex (HPIC) micelles are nanoaggregates obtained by complexation of multivalent metal ions by double hydrophilic block copolymers (DHBC). Solutions of DHBC such as the poly(acrylic acid)-block-poly(acrylamide) (PAA-*b*-PAM) or poly(acrylic acid)-block-poly(2-hydroxyethylacrylate) (PAA-*b*-PHEA), constituted of an ionizable complexing block and a neutral stabilizing block, were mixed with solutions of metal ions, which are either monoatomic ions or metal polycations, such as Al^{3+}, La^{3+}, or Al_{13}^{7+}. The physicochemical properties of the HPIC micelles were investigated by small angle neutron scattering (SANS) and dynamic light scattering (DLS) as a function of the polymer block lengths and the nature of the cation. Mixtures of metal cations and asymmetric block copolymers with a complexing block smaller than the stabilizing block lead to the formation of stable colloidal HPIC micelles. The hydrodynamic radius of the HPIC micelles varies with the polymer molecular weight as $M^{0.6}$. In addition, the variation of R_h of the HPIC micelle is stronger when the complexing block length is increased than when the neutral block length is increased. R_h is highly sensitive to the polymer asymmetry degree (block weight ratio), and this is even more true when the polymer asymmetry degree goes down to values close to 3. SANS experiments reveal that HPIC micelles exhibit a well-defined core−corona nanostructure; the core is formed by the insoluble dense poly(acrylate)/metal cation complex, and the diffuse corona is constituted of swollen neutral polymer chains. The scattering curves were modeled by an analytical function of the form factor; the fitting parameters of the Pedersen's model provide information on the core size, the corona thickness, and the aggregation number of the micelles. For a given metal ion, the micelle core radius increases as the PAA block length. The radius of gyration of the micelle is very close to the value of the core radius, while it varies very weakly with the neutral block length. Nevertheless, the radius of gyration of the micelle is highly dependent on the asymmetry degree of the polymer: if the neutral block length increases in a large extent, the micelle radius of gyration decreases due to a decrease of the micelle aggregation number. The variation of the R_g/R_h ratio as a function of the polymer block lengths confirms the nanostructure associating a dense spherical core and a diffuse corona. Finally, the high stability of HPIC micelles with increasing concentration is the result of the nature of the coordination complex bonds in the micelle core.

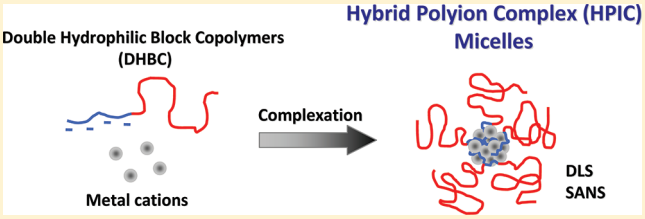

INTRODUCTION

Hybrid polyion complex (HPIC) micelles are organic−inorganic nanoassemblies formed by complexation of multivalent metal ions by double hydrophilic block copolymers (DHBCs). In the past decade, they have received much attention since they are interesting reservoirs of inorganic ions and nanoreactors for inorganic polycondensation reactions. DHBCs are water-soluble copolymers constituted of two blocks of different chemical nature. The interest in these polymers has considerably increased in the past few years; this is due to their numerous potential applications in aqueous medium in diverse areas including drug delivery,[1,2] noble nanoparticle synthesis,[3] colloid stabilization,[4] growth of inorganic crystals such as $CaCO_3$,[5] $BaSO_4$,[6] ZnO,[7] synthesis of metal (hydr)oxide nanoparticles,[8,9] and

Received: November 20, 2011
Revised: January 13, 2012
Published: January 14, 2012

preparation of mesoporous materials[10] using recyclable polymer structuring agents. DHBCs are now well-known as agents of control of mineralization processes: they are used as crystal modifiers for morphosyntheses and bioinspired mineralization processes.[11] In those applications, DHBCs are chosen with one hydrophilic block that can interact with specific inorganic sites (ions, nuclei, or primary particles faces) whereas the other hydrophilic block promotes solubilization in water. In recent reviews,[11] Cölfen et al. described systematic studies of morphogenesis of different minerals by using DHBCs and showed the influence of parameters such as the nature of the polymer functional groups, crystallization sites, temperature, concentrations, and so forth. DHBCs were also used to prepare highly stable hybrid colloids: nanoparticles are obtained by mineralization reactions of HPIC micelles in suspension by following a colloidal preparation route.[8,9] We have previously shown that the use of complexing (anionic)−stabilizing (neutral) hydrophilic block copolymers allowed preparing polymer-protected metal hydroxide nanoparticles: stable Al, La, Cu hydroxide nanoparticles of different shapes (plate-like, elongated, spherical) and controlled sizes were successfully prepared; particles exhibited a core−corona structure with a mineral core protected by water-soluble polymer chains at the surface. We have shown that the true precursors in the nanoparticle formation were the HPIC micelles, whose formation was induced by complexation of the metal cations by the polymer complexing block. Metal hydroxide nanoparticles were obtained by mineralizing the micelle core by adding a basic solution to the HPIC solution. The mineral particle size could be tuned by varying the polymer to metal ion ratio. Moreover, it was the size of the precursor HPIC micelle that determined the minimum size of the mineralized nanoparticles.

The formation of micellar aggregates from DHBCs has been the subject of numerous studies in the literature. One of the main reasons for the growing interest for DHBCs is precisely that the properties of these hydrosoluble block copolymers are tunable by changing environmental parameters such as the pH, the temperature, or the ionic strength, or by interaction with a substrate.[13]

DHBCs micellization process induced by complexation has been more extensively studied in the case of polyelectrolyte-containing DHBCs able to form a complex with an oppositely charged organic compound.[14] The micellar entities are named either polyion complex (PIC micelles)[15] or block ionomer complex (BIC micelles)[16] or complex coacervation core micelles (C3M)[17] depending on the authors. The formation of complex micelles with oppositely charged compounds such as polyelectrolytes[2,10,18] or surfactants[19] has been quite extensively studied; most often studies deal with the case of anionic diblock copolymers mixed with cationic entities. The case of cationic diblock copolymers interacting with DNA was also investigated for drug delivery systems.[20] In those different systems, electrostatic interactions govern the complex structure formation, and it is the entropy gain due to the release of the counterions confined in the electric field of polyelectrolytes that is the main driving force for complex formation. In the literature, the reported micelles are mainly of spherical shape, and they most often present a narrow size distribution. In the case of DHBCs/polyelectrolyte micelles, aggregates are constituted of an electrically neutral core (inter polyelectrolyte complex, IPEC) stabilized by a soluble polymer corona.[15]

The case of DHBC polymer aggregates formed with inorganic polyions or multivalent metal ions has been less investigated. In the literature, few papers deal with such hybrid organic−inorganic complex assemblies.[8,21−23] It was shown that well-defined colloids with a core−corona structure form when mixing neutral-polyelectrolyte DHBCs and metal ions; the colloids are mainly spherical and constituted by the insoluble PAA/cation complex core surrounded by a neutral corona bringing the colloidal stability. In previous papers,[9,22,23] we reported the formation of stable hybrid colloidal suspensions when mixing anionic-neutral DHBCs and multivalent metal cations such as M^{2+}, M^{3+} ions or small condensed charged mineral entities. We studied the case of Cu^{2+}, Al^{3+}, La^{3+} ions and also polycations such as the Keggin tridecamer Al_{13}^{7+}. We showed by SANS and TEM[24] that the hybrid micelles were constituted of a dense spherical core, surrounded by a neutral polymer corona in a good solvent.

In the present paper, we deal specifically with micellar aggregates formed from poly(acrylic acid) (PAA)-*b*-poly(acrylamide) (PAM) or poly(acrylic acid) (PAA)-*b*-poly(2-hydroxyethylacrylate) (PHEA) copolymers and multivalent metal cations. Only the case of asymmetric block copolymers with a functional anionic block smaller than the neutral block is discussed here. The objective is to determine the size and structure dependence of the HPIC micelles as a function of the parameters of the system. This is important since such hybrid micelles are the precursors that act as nanoreactors in mineralization processes and they determine the size of the particles resulting from inorganic polycondensation reactions. The goal is then to be able to tune the size of the precursor HPIC micelles, in order to better control the size of the metal-based nanoparticles that are obtained either by hydroxylation or reduction of the metal cations.

First, we briefly characterize the block copolymers alone, i.e., in the absence of metal cations, by dynamic light scattering. A comparative study of the hydrodynamic behavior of the micellar aggregates and of the copolymers alone in water is presented. Then, hybrid micelles were analyzed by small angle neutron scattering in order to characterize the nanostructure of the objects. Modeling the scattering curves allowed us to determine the critical characteristics of the systems such as the aggregation number, the core size, and the micelle radius of gyration. The influence of the parameters such as the total molecular weight of copolymers, the copolymer block lengths, the nature of the inorganic ion, and finally the polymer concentration on the micelle size and nanostructure is examined and discussed.

EXPERIMENTAL SECTION

Materials and Sample Preparation. $La(NO_3)_3{\cdot}6H_2O$ and $Al(NO_3)_3{\cdot}9H_2O$ (Aldrich) were used as sources of metal ions. Ultrapure deionized water (Milli-Q, Millipore, France) was always used for the preparation of the solutions. Metal-based entities, which are mixed with DHBCs, can be either monoatomic metal ions (Al^{3+}, La^{3+}) or condensed species such as polycationic clusters. Solutions of Al_{13}^{7+} clusters were prepared by controlled hydrolysis of Al^{3+} solutions (0.1 M) with sodium hydroxide solutions (0.3 M) at 90 °C; a prehydrolysis ratio $h_1 = [OH^-]/[M]$ of 2.46 was used.[25] The pH of metal cation solutions and prehydrolysis ratios of ions used in this study are given in Table S1 in Supporting Information. In the present work, two series of block copolymers of different average molecular weights were used. The block copolymers contain the same ionizable block, poly(acrylic acid), and a neutral poly(acrylamide) or poly(2-hydroxyethylacrylate) block. They are noted PAA-*b*-PAM and PAA-*b*-PHEA, respectively. The number-average molecular weights (M_n in g mol^{-1}) are indicated close to each block name as follows: PAA (5000 g·mol^{-1})-*b*-PAM (30 000 g mol^{-1}) is noted PAA_{5000}-*b*-PAM_{30000}. All block copolymers were synthesized by MADIX (standing for macromolecular design by interchange of xanthates),[26]

dx.doi.org/10.1021/la204562t | *Langmuir* 2012, 28, 3773−3782

a controlled radical polymerization developed by Rhodia; the synthesis was described earlier.[27] The chemical structures of block copolymers used in the present work are indicated in Figure S1 in Supporting Information. Concentrations of mother copolymer solutions were of about 5 wt %. The pH of the polymer solutions was adjusted to 5.5, which is close to the apparent pK_a of the PAA block, before mixing polymers and metal ion solutions. At that pH, about half of the acrylic acid functions are neutralized into sodium acrylate groups. The preparation of micelle suspensions is done at room temperature. A given amount of copolymer solution (5 wt %) is added to the solution of metal ions (5×10^{-2} M); the amount depends on the complexation ratio R, which is defined as $R = [COO]/[M]$ where [COO] and [M] are, respectively, the molar concentrations of carboxylic acid groups and metal atoms. Vigorous stirring is continued for 10 min at room temperature. Metal concentration in the final suspensions is adjusted at 10^{-2} M. Depending on R, final polymer concentrations varied between 0.05 and 2.4 wt %.

Characterization. *Dynamic Light Scattering.* The light scattering measurements were performed using a MALVERN spectrogoniometer, AutoSizer 4800, with a 50 mW laser source operating at 532 nm. The accessible scattering angle range is from 30° up to 145°; however, all the scattering measurements were done at 90°. The dynamic light scattering measurements were performed at a constant temperature of 23 °C. The measured normalized time correlation function was analyzed by using the CONTIN algorithm. The values of the hydrodynamic radii were calculated from the decay times using Stokes–Einstein equation: $R_h = k_BT/6\pi\eta D$ where k_B is the Boltzmann constant, T is absolute temperature, η is the solvent viscosity, and D is the coefficient diffusion. All samples were previously filtered through Teflon filters of 0.8 μm pore size. The experimental duration for each experiment was 3–15 min depending on the scattering intensity. The results are given in intensity-averaged hydrodynamic radii.

Small Angle Neutron Scattering. We performed small angle neutron scattering (SANS) measurements at the Laboratoire Léon Brillouin (Saclay, France). SANS spectra $I(q)$ were measured as a function of the amplitude of the scattering vector q. The neutron scattering cross section as a function of the magnitude of the scattering vector q is represented for monodisperse particles by $I(q) = nV^2\Delta\rho^2P(q)S(q)$, where $q = 4\pi/\lambda \sin(\theta/2)$, λ is the wavelength of radiation, θ is the scattering angle, n is the number of particles, V is the volume of the particle, and $\Delta\rho$ is the variation of scattering length density between the particle and the solvent. $P(q)$ is the particle form factor and contains the effects of particle size, shape, and interface with the solvent. $S(q)$ is the structure factor describing the effects of interparticle interactions. For very dilute systems, $S(q) = 1$ and the structure factor can be neglected.

The coherent scattering length, molecular volumes, and coherent scattering density of the different species used in this study are given in Table S2 in Supporting Information. We have compared the scattering length densities of different scattering systems, and D_2O has been chosen in order to minimize the incoherent background from hydrogen. Indeed, the difference of neutron scattering length density between the polymer chains and the deuterated solvent yields a high contrast.[28] All the metal ion suspensions were also prepared in D_2O. Al_{13} clusters were then synthesized in D_2O at 90 °C, and the obtained $Al_{12}(AlO_4)(OD)_{24}(D_2O)_{12}^{7+}$ species have a scattering length density similar to that of D_2O.

The samples were put in quartz cells (HELLMA) with a width of 2 mm. The SANS spectra of H_2O, used for calibration, were measured with a 1 mm thick quartz cell. A q-range from 0.004 to 0.5 Å^{-1} was covered by collecting data at two distances d = 1 and 3 m, with respective incident neutron wavelengths of 5 and 10 Å. The gyration radii of micellar aggregates were determined by fitting the scattering profiles with the Guinier approximation $I(q) = I(0)\exp(-q^2R_g^2/3)$; the Zimm approximation $I(q) = I(0)/(1+q^2R_g^2/3)$ was used only in the case of block copolymers alone.

RESULTS AND DISCUSSION

Copolymers in Water. Before studying the HPIC micelles between DHBCs and metal ions, the characteristics of the polymers alone in water were examined. This was necessary in order to determine the copolymer conformations in the absence of metal ions and then to study the influence of the metal ion complexation. It is well-known that hydrogen bonds may form between poly(acrylamide) and poly(acrylic acid) leading to chain aggregation, and complex coacervation may occur depending on the pH, the concentration, and the temperature of the aqueous solution.[29] It was then necessary to examine the polymer behavior in the present conditions. Aqueous solutions of block copolymers were prepared at a 2 wt % concentration and were analyzed at pH 5.5. All polymer solutions appear clear.

Here, the solubility of a series of PAA-*b*-PAM block copolymers of different molecular weights is studied by dynamic light scattering in water at pH 5.5. Hydrodynamic radii R_h were determined and listed in Table 1. Figure 1 shows the variation

Table 1. Average Values of Hydrodynamic Radii R_h Obtained for PAA-*b*-PAM Block Copolymers in Water at T = 23 °C and pH 5.5

copolymer	M_{tot} (g mol^{-1})	R_h (nm)
PAA_{1000}-*b*-PAM_{10000}	11 000	3.7
PAA_{3000}-*b*-PAM_{10000}	13 000	4.5
PAA_{6000}-*b*-PAM_{10000}	16 000	4.9
PAA_{10000}-*b*-PAM_{10000}	20 000	6.1
PAA_{15000}-*b*-PAM_{10000}	25 000	6.8
PAA_{3000}-*b*-PAM_{30000}	33 000	6.9
PAA_{5000}-*b*-PAM_{30000}	35 000	5.0
PAA_{5000}-*b*-PAM_{60000}	65 000	10.4

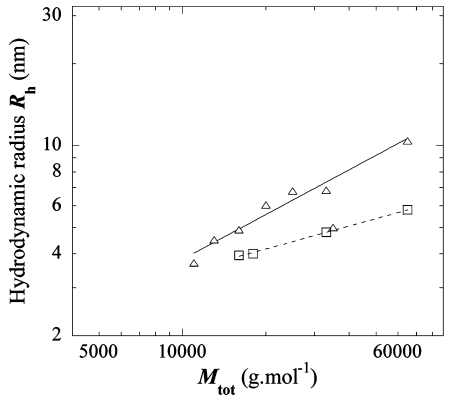

Figure 1. Evolution (log–log scale) of hydrodynamic radii R_h (nm) as a function of the total molecular weight of PAA-*b*-PAM copolymers at pH 5.5 (Δ) and at pH 3 (□). The list of copolymers is given in Table 3. The solid line and the dashed lines correspond, respectively, to the scaling law $R_h \sim M_{tot}^{0.55}$ and $R_h \sim M_{tot}^{0.3}$.

of R_h as a function of the total molecular weight of the polymer in a log–log scale. When the polymer molecular weight increases, hydrodynamic radii increase following a power law: $R_h \sim M_{tot}^{0.55}$. The value of the power exponent is very close to that predicted for neutral polymers in a good solvent.[30] These results demonstrate that the PAA-*b*-PAM polymers have the same conformation in water whatever the molecular weight, and that no self-assembly phenomenon between polymers due to intramolecular or intermolecular hydrogen bonding was

dx.doi.org/10.1021/la204562t | Langmuir 2012, 28, 3773–3782

present. Moreover, the fact that the power law in $M_{tot}^{0.55}$ is valid here for the eight block copolymers of different asymmetry degrees suggests that the presence of the small PAA block does not lead to a noticeable change of the overall copolymer conformation compared to totally neutral polymers. Only the hydrodynamic radius of the PAA_{5000}-*b*-PAM_{30000} copolymer does not fit in the power law curve.

On the other hand, when the series of copolymers is analyzed at pH close to 3 (initial pH), the hydrodynamic radii are much smaller (see Figure 1), showing that, in dilute conditions, intramolecular hydrogen bonds within each diblock polymer chain lead to a compact conformation. This phenomenon is also revealed by the lower exponent value in the power law $R_h \sim M_{tot}^{0.3}$, which is observed at this low pH. By increasing the pH from 3 to 5.5, the polymer chains swell suggesting that hydrogen bonds progressively disappear. In conclusion, above pH 5, the present DHBCs behave as very soluble polymers in water, and no self-assembly is observed. The present results are consistent with some previous results[23] obtained on a series of PAA-*b*-PHEA polymers by SANS, showing that PAA-*b*-PHEA polymers at pH 5.5 behave as water-soluble macromolecules with excluded volume effects.

Formation of Hybrid Polyion Complex Micelles from DHBCs and Metal Ions. In the following, mixtures of DHBCs and metal ions are studied. A given amount of DHBCs solution at pH 5.5 was added to cation solutions keeping a ratio *R* equal to 1. The pH of inorganic solutions varies with the cation nature and the prehydrolysis ratio of the metal ions (see Experimental Section).

It is well-known that mixing anionic polyelectrolytes and multivalent cations leads to macroscopic phase separation if specific interactions between cations and polyions exist.[31] On the contrary, when anionic-neutral double hydrophilic block copolymers (PAA-*b*-PAM or PAA-*b*-PHEA) and multivalent cations were mixed, no macroscopic phase separation occurred; nevertheless, colloidal objects were formed.[9] It was also observed that the mixing was accompanied by a decrease of the pH and an increase of the total conductivity. These variations, which are characteristic of the complexation reaction between DHBCs and inorganic species, will be further studied in a forthcoming paper.

The aspect of the suspensions depends on the molecular weight of the copolymer, its asymmetry, and the nature of the cations. For instance, a solution prepared with PAA_{1000}-*b*-PAM_{10000} and Al^{3+} was clear, whereas a solution prepared with PAA_{5000}-*b*-PAM_{30000} and Al^{3+} was slightly opalescent. Also, suspensions become more turbid when the cation size increases. Complexation between polyelectrolyte-neutral DHBC and multivalent cations leads to a phase separation that remains limited at a nanoscopic scale, since the growth of the polyion/cation complex is controlled by the presence of the long neutral polymer chains forming a stabilizing corona around the complex.

Hydrodynamic Sizes of the HPIC Micelles as a Function of the Polymer Block Lengths and of the Cation. The HPIC micelles were characterized by dynamic light scattering (DLS). Before analyzing raw DLS results, it was necessary to make sure that the dynamics of the colloids was purely diffusive and then that, diffusion coefficients, *D*, and hydrodynamic radii, R_h, of the colloidal objects could be determined in the chosen conditions. The dependence of the correlation time extracted from the autocorrelation functions, $g^{(1)}(q,t)$, recorded for a range of scattering angles from 30° to 130° corresponding to a range of wave vectors *q* from 8.13×10^{-3} to 2.85×10^{-2} nm^{-1}, with the wave vector (τ varies as q^{-2}), demonstrates that the dynamics of PAA_{5000}-*b*-PAM_{30000}/Al_{13}^{7+} nanoaggregates is purely diffusive, and this allows the determination of hydrodynamic radii (see Figure S2 in Supporting Information).

In Table 2, the intensity-averaged values of R_h for different mixtures of PAA-*b*-PAM and PAA-*b*-PHEA DHBCs and multivalent cations, at a metal complexation ratio *R* equals to 1, are reported. We had previously shown[9,22] (in the case of La^{3+} cation) that the size of PAA-*b*-PAM based micelles did not vary with the degree of complexation *R*, for ratios *R* ranging from 0.1 to 3. The same observations were obtained again here with Al_{13}^{7+} polycations and different PAA-*b*-PAM and PAA-*b*-PHEA DHBCs (see Figure S3 in Supporting Information). Moreover, the polydispersity index remained low, on the whole range of *R* values. For those reasons, all of the following experiments were performed at a given ratio, *R* = 1. For highly asymmetric block copolymers, we observe that the size of the nanoaggregates increases with the total molecular weight. Depending on inorganic cations, the size varies from 7 to 45 nm when the total molecular weight varies from 11 000 g mol^{-1} to 65 000 g mol^{-1}. In Figure 2, hydrodynamic radii of the complex micelles are plotted as a function of the polymer molecular weights in a log−log scale. The R_h values of colloids formed between DHBCs and metal ions are 3−4 times higher than the hydrodynamic radii of copolymers alone at pH = 5.5. As for copolymers alone (see Figure 1), the hydrodynamic radii of the aggregates increase with increasing molecular weights following a power law $R_h \sim M_{tot}^{\beta}$. Concerning HPIC micelles formed between PAA-*b*-PAM and Al^{3+}, La^{3+}, or Al_{13}^{7+} cations, the power exponent β equals 0.56, 0.70, and 0.58, respectively. These values are close to those obtained for DHBCs without added cations (see Figure 1). This result shows that the hydrodynamic properties of these objects (micelles and copolymers) are mainly controlled by a major contribution of neutral polymer chains, which are swollen in water.

Table 2. Hydrodynamic Radii of Colloidal Nanoaggregates Obtained from DHBC (PAA-*b*-PAM or PAA-*b*-PHEA) and Multivalent Cations with a Complexation Ratio *R* = 1

		hydrodynamic radii R_h (nm)		
copolymer	M_{tot} (g.mol^{-1})	Al^{3+}	La^{3+}	Al_{13}^{7+}
PAA_{1000}-*b*-PAM_{10000}	11 000	7.4	11.9	14.0
PAA_{3000}-*b*-PAM_{10000}	13 000	15.6	12.3	17.8
PAA_{6000}-*b*-PAM_{10000}	16 000	19.3	24.5	35.0
PAA_{3000}-*b*-PAM_{15000}	18 000			23.5
PAA_{3000}-*b*-PAM_{30000}	33 000	20.4	25.0	27.5
PAA_{5000}-*b*-PAM_{30000}	35 000	31.5	27.3	43.0
PAA_{5000}-*b*-PAM_{60000}	65 000	39.5	39.5	44.0
PAA_{900}-*b*-$PHEA_{9200}$	10 100			11.0
PAA_{1900}-*b*-$PHEA_{8200}$	10 100		18.8	20.5
PAA_{2800}-*b*-$PHEA_{11100}$	13 900		23.5	23.5

Table 2 shows that the hydrodynamic radius changes with the nature of the cation. Aggregates formed with Al_{13}^{7+} are bigger than those formed with Al^{3+}, while changing Al^{3+} for La^{3+} leads to a smaller change of R_h. It also appears that increasing the PAA block length in a large extent, while keeping the size of the neutral block constant, leads to a considerable increase of the averaged R_h; this is clear in the $PAA_{n\times1000}$-*b*-PAM_{10000} series with *n* = 1, 3, and 6. This cannot be simply explained by an increase of the size of a spherical core when the

dx.doi.org/10.1021/la204562t | *Langmuir* 2012, 28, 3773−3782

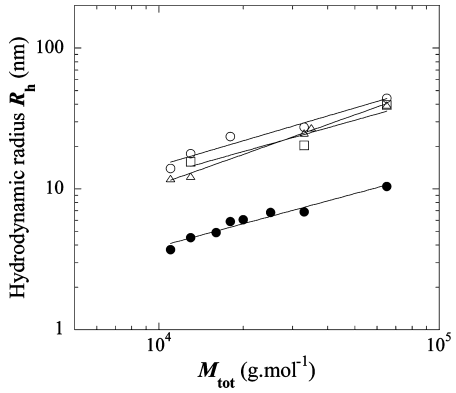

Figure 2. Hydrodynamic radii R_h (nm) of colloidal aggregates formed between PAA-*b*-PAM copolymers and multivalent cations at R = 1: Al^{3+} (□), La^{3+} (Δ), and Al_{13}^{7+} (○). The cation concentration is 10^{-2} M. The copolymers used are listed in Table 1. The full circles (●) correspond to copolymers alone at pH 5.5 presented in Figure 1.

PAA block is larger. We have to consider the change of the asymmetry degree of the copolymer that can be defined as the ratio between the average molecular weight of the neutral block, $M_{w,neutral}$, and the molecular weight of the complexing block, $M_{w,complexing}$. A high asymmetry degree corresponds to a block copolymer with a small polyelectrolyte block and a large neutral block. In the $PAA_{n\times1000}$-*b*-PAM_{10000} series, when $M_{w,neutral}/M_{w,complexing}$ varies from 10 to 1.7, R_h increases from 14 to 35 nm. The same trend is observed with PAA-*b*-PHEA polymers: when the asymmetry degree decreases from 10.2 (PAA_{900}-*b*-$PHEA_{9200}$) to 4.3 (PAA_{1900}-*b*-$PHEA_{8200}$), the intensity-averaged radius increases from 11 to 21 nm, while the polymer total molecular weight remains constant. These results demonstrate that the hydrodynamic radius is strongly affected by the size of the complexing block and by the asymmetry degree of the polymer.

On the other hand, increasing the neutral block length while keeping the size of the ionic block constant also leads to an increase of R_h. In the series of complexes between Al_{13}^{7+} and PAA_{3000}-*b*-$PAM_{n\times10000}$ (with n = 1, 1.5, and 3), R_h increases from 17 to 28 nm when n increases from 1 to 3 (correspondingly, the asymmetry degree varies from 3.3 to 10). As the PAM block is very soluble in water, an increase of its molecular weight leads to a large increase of the R_h.

In conclusion, the present results show that aggregation of DHBCs induced by complexation of inorganic cations leads to the formation of stable colloids with the following properties: Their hydrodynamic radii vary with the total molecular weight of the copolymer following power laws similar to that of corresponding neutral soluble polymers ($R_h \sim M^{0.6}$). The micelle size depends on the nature of the inorganic cation and on the molecular weights of the blocks. It varies strongly with the asymmetry degree of the polymer; it is more sensitive to a change of the complexing block length than to a change of the stabilizing block.

Core−Corona Nanostructure of the HPIC Micelles. Small angle neutron scattering experiments were carried out in order to characterize the nanostructure of the complex micelles as a function of the copolymer composition and the nature of the metal cation. Radii of gyration of the colloids were determined, and the scattering data were fitted using a model in order to determine the aggregation number and the core radius of the micelles. The radii of gyration of the chains in the corona were also estimated.

When mixing double hydrophilic block copolymers and multivalent cations, a considerable change of the scattered intensity profile was obtained compared to that of the copolymer alone.[23] This is due to polymer aggregation upon addition of oppositely charged multivalent ions. Figure 3 presents the SANS curves of nanoaggregates formed between Al_{13}^{7+} polycations and PAA-*b*-PHEA polymers (PAA_{900}-*b*-$PHEA_{8200}$, PAA_{1900}-*b*-$PHEA_{8200}$, PAA_{2800}-*b*-$PHEA_{11100}$) on one hand and PAA-*b*-PAM polymers (PAA_{1000}-*b*-PAM_{10000}, PAA_{3000}-*b*-PAM_{10000}) on the other hand, with a same complexation ratio, R = 1. The scattered intensities were normalized by the polymer weight concentration. At high q values, all the curves follow the same power law suggesting that all nanoaggregates, PAA-*b*-PHEA/Al_{13} and PAA-*b*-PAM/Al_{13}, have similar interfaces with the solvent. In this q value domain, the scattered intensities vary as $q^{-\alpha}$, where α varies between 1.7 and 2. The value of the exponent is a signature of the diffuse and solvated character of the polymer corona constituted of neutral chains swollen in water. The power laws obtained for nanoaggregates and copolymers alone are similar and indicate that the conformation of polymer neutral chains is similar. This is in agreement with DLS results, which show that nanoaggregates and DHBCs have a similar hydrodynamic behavior. In the intermediate q range (0.02−0.06 Å^{-1}), scattered intensities decrease sharply, following a power law in $q^{-3.9}$. This observation shows that the micelle core is compact and homogeneous and possesses a sharp and well-defined interface with the corona.

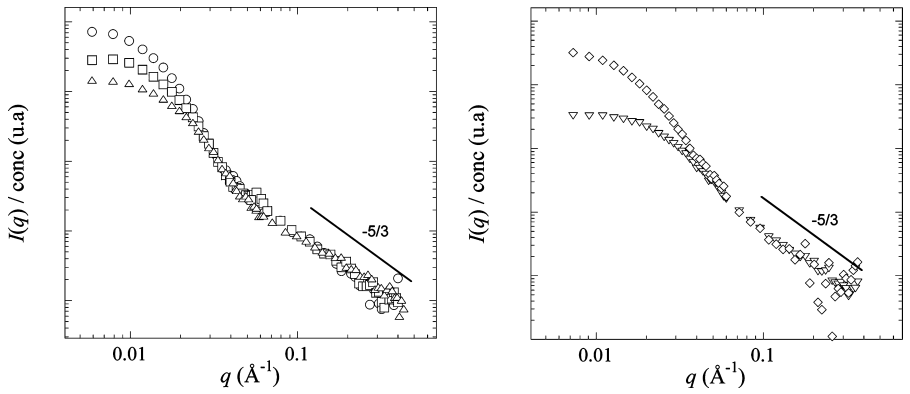

Figure 3. Profiles of scattered intensities normalized at the same polymer concentration for the nanoaggregates: (left) (Δ) PAA_{900}-*b*-$PHEA_{8200}$/Al_{13}, (□) PAA_{1900}-*b*-$PHEA_{8200}$/Al_{13}, and (○) PAA_{2800}-*b*-$PHEA_{11100}$/Al_{13}; and (right) (▽) PAA_{1000}-*b*-PAM_{10000}/Al_{13} and (◇) PAA_{3000}-*b*-PAM_{10000}/Al_{13}. The complexation ratio is the same, R = 1.

dx.doi.org/10.1021/la204562t | *Langmuir* 2012, 28, 3773−3782

At low q values, in the Guinier region, the radii of gyration $R_{g,a}$ of the aggregates are obtained by the Guinier approximation. Table 3 reports the values of $R_{g,a}$, R_h, and the $R_{g,a}/R_h$ ratios.

Table 3. Radii of Gyration $R_{g,a}$, Hydrodynamic Radii R_h, and Ratio of Nanoaggregates $R_{g,a}/R_h$ Formed with PAA-*b*-PHEA and PAA-*b*-PAM Copolymers of Different Block Lengths and the Polycation Al_{13}

sample	M_{tot} (g.mol^{-1})	$R_{g,a}$ (nm)	R_h (nm)	$R_{g,a}/R_h$
PAA_{900}-*b*-$PHEA_{9200}/Al_{13}$	10 100	9.0	11.0	0.81
PAA_{1900}-*b*-$PHEA_{8200}/Al_{13}$	10 100	10.7	20.5	0.52
PAA_{2800}-*b*-$PHEA_{11100}/Al_{13}$	13 900	12.6	23.5	0.53
PAA_{1000}-*b*-PAM_{10000}/Al_{13}	11 000	6.2	14.0	0.44
PAA_{3000}-*b*-PAM_{10000}/Al_{13}	13 000	10.5	17.8	0.59
PAA_{3000}-*b*-PAM_{15000}/Al_{13}	15 000	11.8	23.5	0.50
PAA_{3000}-*b*-PAM_{30000}/Al_{13}	33 000	10.7	27.5	0.39

In the case of PAA-*b*-PHEA based nanoaggregates, the radius of gyration increases with the length of the polyelectrolyte block. In the case of polymers PAA_{1000}-*b*-PAM_{10000} and PAA_{3000}-*b*-PAM_{10000}, the radius of gyration increases from 6.2 to 10.5 nm, when the polyelectrolyte chain length is multiplied by 3. Moreover, $R_{g,a}$ values weakly depend on the length of the neutral block. Indeed, in the series of Al_{13} complex micelles with PAA_{3000}-*b*-$PAM_{n\times10000}$ (with n = 1, 1.5, and 3), in which the size of the polyelectrolyte block is kept constant while the neutral block is increased (by a factor of 3), $R_{g,a}$ only varies from 10.5 to 11.8 nm. Actually, when the PAM molecular weight increases from 10 000 to 15 000, $R_{g,a}$ slightly increases from 10.5 to 11.8, due to the small contribution of the corona chains to $R_{g,a}$. However, when the PAM length increases further (from 15 000 to 30 000 g/mol), $R_{g,a}$ decreases down to 10.7: this is due to the decrease of the core size upon increasing the volume of the soluble corona chains. This behavior is similar to what is known for the case of classical amphiphilic block copolymers; i.e., when the asymmetry degree increases, the aggregation number decreases, leading to a decrease of the core size. In conclusion, the radii of gyration of the nanoaggregates strongly vary with the length of the polyelectrolyte block and, to a much smaller extent, with the length of the neutral chains. The low values obtained for the $R_{g,a}/R_h$ ratio are discussed further in the paper.

SANS Modeling. The SANS analysis has shown that the HPIC micelles are constituted of a dense homogeneous core ($I \sim q^{-3.9}$ in the intermediate q range) and a corona made of solvated polymer chains ($I \sim q^{\alpha=-1.7\text{ to }-2}$ in the high q range). So, in order to model the micelle SANS curves, we used a model that gives the same dependence of the scattered intensity versus the wave vector q, namely in q^{-4} and q^{-2}, and which renders a core−corona structure. We used the Pedersen's model, which is an analytical function developed for form factors of spherical micelles of amphiphilic block copolymers.[32,33] This model allows describing spheres of homogeneous density surrounded by Gaussian chains attached to it. The analytical expression of the model contains four terms: the self-correlation of the core, the self-correlation of the chains, the interference cross-term between the core and chains, and the interference cross-term between chains. In a classical amphiphilic block copolymer micelle, the core is formed of polymer chains in a bad solvent, whereas polymer chains in a good solvent constitute the corona of the micelle. In the present case, the core is formed by the insoluble PAA/cation complex, while the soluble PAM or PHEA chains constitute the corona. The fitting parameters are the radius R_s of the dense sphere (core), the gyration radius $R_{g,c}$ of neutral polymer chains (corona), and the aggregation number N_{agg} (number of block copolymers per aggregate). We expect to observe a slight difference between the model and the experimental curves in the domain of high q values because the Pedersen's model uses Gaussian statistic chains for describing the micelle corona. Indeed, in amphiphilic block copolymer micelles, the contribution of the corona is expressed at high q values as a power law $I \sim q^{-1/\nu}$ where ν is the Flory exponent.[30] For Gaussian statistic chains, $\nu = {}^1/_2$ and the intensity varies as q^{-2} at high q values, whereas for chains in a good solvent (with excluded volume), ν equals ${}^3/_5$ and the intensity decreases as $q^{-5/3}$. The same analytical form was used for fitting form factors of all the nanoaggregates obtained here between PAA-*b*-PHEA DHBCs of different compositions and various multivalent cations: Al^{3+}, La^{3+}, and Al_{13}^{7+}. Here, we precisely examine the case of the Al_{13}^{7+} polycation and the influence of the composition of the block copolymer on the micelle structure.

Figure 4 displays the model curves for a PAA-*b*-PHEA/Al_{13} series with polymers of different molecular weights. In the whole range of wave vector q, the Pedersen's model allowed us to correctly fit the experimental data. At low q values, the model curve perfectly describes the dense core of the HPIC micelles formed by the insoluble PAA/Al_{13} complex. In the intermediate q range between 0.06 and 0.15 Å^{-1}, oscillations in the model curves are due to the form factor of the spheres, which are considered as monodisperse. The slight discrepancy at high q values is due to the fact that Pedersen's model neglects the excluded volume effects between the chains, as was mentioned earlier. The values of the fit parameters obtained with the model are given in Table 4. The core radius, R_s, increases with the molecular weight of the PAA block, which is consistent with an increase of the size of the insoluble PAA/Al_{13} complex. We also observe that R_s values are close to the experimental radii of gyration of nanoaggregates $R_{g,a}$ (Table 3). This means that the dense core represents the main contribution to the gyration radius of the nanoaggregate: this is consistent with the diffuse character of the polymer corona.

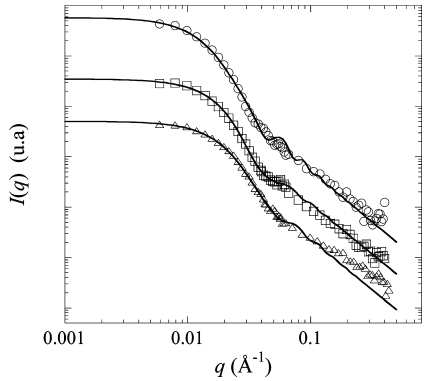

Figure 4. Comparison of the SANS profiles between experimental data and the model: (Δ) PAA_{900}-*b*-$PHEA_{8200}/Al_{13}$, (□) PAA_{1900}-*b*-$PHEA_{8200}/Al_{13}$, and (○) PAA_{2800}-*b*-$PHEA_{11100}/Al_{13}$ at R = 1. The full lines correspond to the model. The intensities have been shifted for clarity.

The close values of R_s and $R_{g,a}$ can partly explain why $R_{g,a}/R_h$ ratios have low values. The ratio $R_{g,a}/R_h$ has often been used in the literature in order to provide some qualitative information about the structure of colloids or to estimate the degree of

dx.doi.org/10.1021/la204562t | Langmuir 2012, 28, 3773−3782

Table 4. List of Parameters Used in the Fitting Neutron Scattering Data of PAA-*b*-PHEA/Al_{13} (R = 1) Systems: Aggregation Number N_{agg}, Core Micelle Radius R_s, Gyration Radius of Gaussian Chains $R_{g,c}$

sample	M_{tot} (g mol^{-1})	M_{PHEA}/M_{PAA}	N_{agg}	R_s (nm)	$R_{g,c}$ (nm)
PAA_{900}-*b*-$PHEA_{9200}/Al_{13}$	10 100	10.2	6−7	8.0	3.8
PAA_{1900}-*b*-$PHEA_{8200}/Al_{13}$	10 100	4.3	11	9.0	3.5
PAA_{2800}-*b*-$PHEA_{11100}/Al_{13}$	13 900	3.9	15	10.5	5.5

swelling of a micelle corona.[34] For PAA-*b*-PHEA/Al_{13} and PAA-*b*-PAM/Al_{13} HPIC micelles, the experimental values of $R_{g,a}/R_h$ ratios vary from 0.39 to 0.59 (except in one case, with copolymer PAA_{900}-*b*-$PHEA_{9200}$). Most of the values are smaller than the theoretical value known for homogeneous dense spheres: $R_{g,a}/R_h \sim (3/5)^{1/2} \sim 0.77$. This may be explained by the fact that the nanoaggregates have a core−corona structure with a small core and a highly swollen corona. Indeed, $R_{g,a}$ is heavily weighted by the dense core, while the neutral chains, which form the corona, are highly swollen by water.[35] Neutral chains bring a minor contribution to $R_{g,a}$ (even if they are longer than PAA chains), whereas they bring a major contribution to R_h. The values of $R_{g,a}/R_h$ are in good agreement with the fact that the PAA-*b*-PHEA/Al_{13} or PAA-*b*-PAM/Al_{13} systems form core−corona structures.

Figure 5 presents the variation of the $R_{g,a}/R_h$ ratio as a function of the PAM block molecular weight in the series

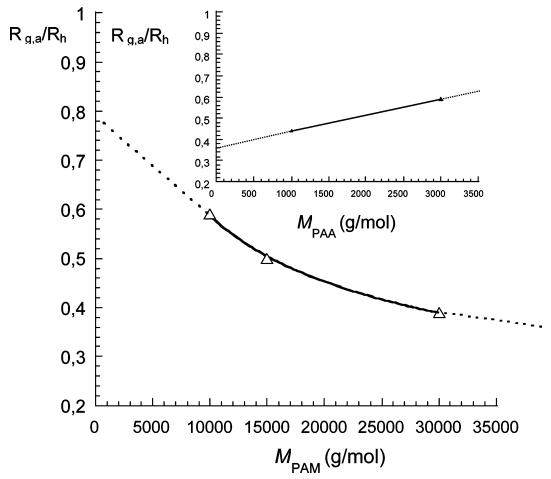

Figure 5. Variation of $R_{g,a}/R_h$ as a function of the PAM block length in the series PAA_{3000}-*b*-$PAM_{(10000,\ 15000,\ and\ 30000)}$ and as a function of the PAA block length in the series $PAA_{(1000,\ 3000)}$-*b*-PAM_{10000}.

PAA_{3000}-*b*-$PAM_{n\times10000}$ (with n = 1, 1.5, and 3), where the PAA block length is constant. When the PAM block length is extrapolated to zero (corresponding to a dense core without corona), a higher $R_{g,a}/R_h$ value close to 0.7−0.8 is obtained. This value is close to 0.77, suggesting that the complex core can be assimilated to a dense sphere. When the PAM block is extrapolated to a very high value, the micelle can be compared to a star like micelle and very low values of $R_{g,a}/R_h$ are obtained, which are consistent with the lower values observed for highly swollen objects (close to 0.3). The variation of $R_{g,a}/R_h$ was also studied as a function of the PAA block length in the series $PAA_{(1000,3000)}$-*b*-PAM_{10000} (inset in Figure 5). It shows a consistent variation: when the PAA block length becomes infinite, R_g/R_h tends toward high values close to 0.7−0.8 (it is expected that it levels off at that value for very long PAA chains); this is consistent with a core size becoming infinite compared to the corona, leading to a R_g/R_h value characteristic of spheres. On the other hand, when the PAA block length becomes very small, the object tends to be a starlike micelle and a low value of R_g/R_h is then expected (around 0.3−0.35). Both variations of R_g/R_h as a function of PAA and PAM block lengths confirm that the micelle core can be assimilated to a dense sphere and that the neutral chains form a diffuse corona.

Table 4 also shows that the radii of gyration $R_{g,c}$ of the corona polymer chains, deduced from the Pedersen's model, increase with the molecular weight of the PHEA neutral blocks: The values are also very close to the radii of gyration determined for block copolymers alone (Zimm approximation). This suggests that (i) in PAA-*b*-PHEA copolymer solutions, the contribution of the PAA block to the radius of gyration is small, and (ii) in PAA-*b*-PHEA/Al_{13} micelles, the PHEA polymer chains forming the corona are in a good solvent and may be slightly stretched.

An interesting point concerns the variation of the aggregation number N_{agg} of the PAA-*b*-PHEA/Al_{13} systems, obtained from the Pedersen's fitting curves. It is observed (Table 4) that the micelle aggregation number, N_{agg}, increases when the asymmetry degree of the block copolymers decreases: when the M_{PHEA}/M_{PAA} ratio decreases from 10.2 down to 3.9, the micelle aggregation number increases from 6 to 15. Indeed, when a block copolymer with a high asymmetry degree is mixed with inorganic cations, the volume occupied by the soluble chains is much bigger than that of the insoluble compact hybrid complex: Then, the interface that spontaneously forms between the core and the corona exhibits a high curvature, leading to a small aggregation number. On the other hand, when the core size increases with respect to the corona, the curvature of the spontaneous interface decreases and leads to an increase of the aggregation number. The variations of N_{agg} observed here are consistent with the variations of R_h, which are commented on previously in the paper. Moreover, they are qualitatively similar to what is well-known for conventional amphiphilic polymer systems.[36]

In conclusion to this part, the form factors of the HPIC micelles have been described using a model, which had been applied to the case of conventional amphiphilic block copolymer micelles. The overall agreement between the model curves and SANS experimental data is quite good, especially concerning the core of the nanoaggregates at low q values and, also, in the intermediate q range, which characterizes the interface between the core and the corona. At high q values, some slight discrepancies are observed in relation with excluded volume effects, which are not taken into account in the analytical function, but they do not prevent us from determining the fitting parameters, which allow a fine characterization of the systems.

Effect of the Concentration on HPIC Micelle Suspensions. The objective was to study the influence of the concentration of the system on the structure of HPIC micelles. Suspensions of PAA_{5000}-*b*-PAM_{30000}/Al_{13}^{7+} nanoaggregates were prepared as indicated in the experimental part ([Al] = 10^{-2} M). Then, they were freeze-dried, and the powders were redispersed in deuterated water for preparing concentrated solutions at the following polymer concentrations: 10, 20, and 31 wt %. The obtained concentrated suspensions were perfectly homogeneous, and they appeared clear and were very stable with time. The SANS curves are presented in Figure 6; they

dx.doi.org/10.1021/la204562t | Langmuir 2012, 28, 3773−3782

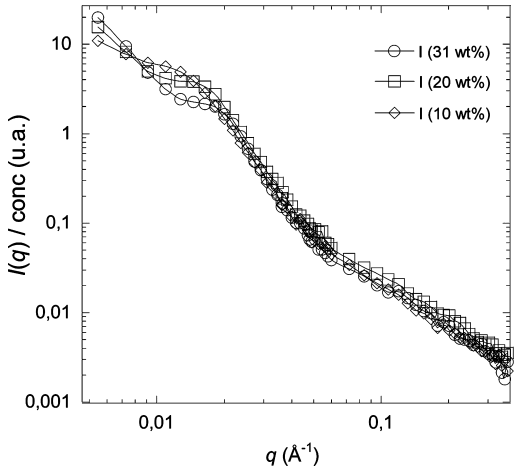

Figure 6. Profiles of scattered intensities I/C (normalized at the same polymer concentration) as a function of q of Al_{13}^{7+}/ PAA_{5000}-*b*-PAM_{30000} nanoaggregate suspensions at three polymer weight concentrations. The lines are only to guide the eye.

were normalized by the polymer concentration. An increase in the polymer concentration leads to an increase of the scattered intensity (I/C) at low q values, suggesting attractive forces between the HPIC micelles at concentrations higher than 10 wt %. Moreover, the scattered intensity increases further as the concentration increases. It is also noticeable that the domain of the SANS curve at q higher than 0.02 $Å^{-1}$ does not change with concentration, showing that the interface between the core and the corona and the interface between the corona and the solvent do not change when the concentration increases: the neutral polymer corona remains in a diffuse configuration as shown by the constant power law exponent ($q^{-1.7}$). The high stability of the HPIC micelles as a function of the concentration is certainly due to the nature of the interaction (coordination complexes) at the origin of the formation of the core. Besides, we have observed that the micelles were not sensitive to dilution or to an increase of the ionic strength (up to 2.5 M); this is due to the high stability of the metal coordination bonds within the core. It can be concluded that HPIC micelles formed between DHBC and metal cations or polycations keep an isotropic shape and the same aggregation degree in highly concentrated aqueous solutions.

CONCLUSION

Hybrid polyion complex micelles were obtained by assembly of water-soluble anionic−neutral block copolymers and inorganic multivalent ions. Inorganic entities are preferentially small, such as inorganic metal ions (Al^{3+}, La^{3+}) or polycationic clusters (Al_{13}^{7+}). With asymmetry degrees higher than 1 (varying between 3 and 12), the copolymers present a complexing to stabilizing balance that is favorable to the formation of stable HPIC micelles. Metal complexation reactions between the polyacrylate block and the metal ions are at the origin of DHBC aggregation, while the good solubility of the neutral polymer blocks ensures the colloidal stability of the HPIC micelles. Core−corona objects are obtained, and the insoluble core is formed by the polyacrylate/cations complex and the corona by the neutral polymer blocks. The micelle hydrodynamic radii vary as a function of the total molecular weight of the polymer, following a power law with a power exponent close to 0.6. The diffusion behavior of the nanoaggregates is governed by a major contribution of the long neutral chains in a good solvent. Moreover, R_h values are particularly sensitive to an increase of the complexing block length, when keeping the neutral block constant, and the effect is all the more pronounced as the asymmetry degree decreases down to values close to 3. The effect is also important when decreasing the neutral block length while maintaining the complexing block length constant. Radii of gyration are more sensitive to the variation of the aggregate core size, and then to the PAA block molecular weight. An increase of the neutral block molecular weight does not lead to a drastic change of $R_{g,a}$; however, above a critical value, it considerably influences the soluble/insoluble balance of the HPIC micelle, and it can induce a decrease of $R_{g,a}$, due to a core size decrease. Then, $R_{g,a}$ and R_h values exhibit different variation laws when changing copolymer block lengths. The high density of the small insoluble complex core and the highly swollen character of the neutral corona lead to small values of the $R_{g,a}/R_h$ of the HPIC micelles. It should be noted that $R_{g,a}/R_h$ increases with the length of the complexing block while it decreases with the length of the neutral block, revealing that the behavior of HPIC micelles concerning their size or aggregation number variations is similar to what is classically observed with permanent amphiphilic systems.[35] Finally, increasing the concentration of micelle suspensions leads to very stable and more viscous suspensions, which are more concentrated solutions of the original isotropic objects. This underlines the high stability of the HPIC micelles.

In conclusion, the present system, which results from a complex between two originally water-soluble entities, can be considered as an *induced* amphiphilic system, since the two components (the PAA/cation complex, on one hand, and the neutral chains, on the other hand) have very different affinities for the aqueous solvent. The association mode utilized here is complexation by formation of metal coordination bonds. A further comparison between these hybrid *induced* amphiphilic systems, and the most extensively studied conventional block copolymer micelle systems in aqueous medium (which are the ones using the hydrophobic attraction as the driving force for segregation) is in progress. The present results already show some similarities between the two families concerning the dependence of the size or aggregation numbers with the polymer block lengths. Finally, the metal−DHBC complex systems are highly versatile and tunable systems since the characteristics (chemical nature, size, and charge) of both components can be varied independently.

ASSOCIATED CONTENT

Supporting Information

Additional tables and figures. This material is available free of charge via the Internet at http://pubs.acs.org.

AUTHOR INFORMATION

Corresponding Author

*Phone: +33 467 163 465. Fax: +33 467 163 470. E-mail: corine.gerardin@enscm.fr.

Notes

The authors declare no competing financial interest.

ACKNOWLEDGMENTS

The authors thank L. Auvray for his help with setting up the neutron scattering experiments, at the Laboratoire Léon Brillouin, Saclay, France, and D. Hourdet for valuable discussion.

REFERENCES

(1) Harada, A.; Kataoka, K. *Prog. Polym. Sci.* **2006**, *31*, 949−982. Lee, Y.; Kataoka, K. *Soft Matter* **2009**, *5*, 3810−3817.

(2) Boudier, A.; Aubert-Pouëssel, A.; Gérardin, C.; Devoisselle, J. M.; Bégu, S. *Int. J. Pharm.* **2009**, *379*, 212−217. Boudier, A.; Aubert-Pouëssel, A.; Louis-Plence, P.; Quentin, J.; Gérardin, C.; Jorgensen, C.; Devoisselle, J. M.; Begu, S. *Drug Dev. Ind. Pharm.* **2009**, *1*, 1−9. Boudier, A.; Aubert-Pouëssel, A.; Louis-Plence, P.; Gérardin, C.; Jorgensen, C.; Devoisselle, J. M.; Bégu, S. *Biomaterials* **2009**, *30*, 233−241.

(3) Bronstein, L. M.; Sidorov, S. N.; Gourkova, A. Y.; Valetsky, P. M.; Hartmann, J.; Breulmann, M.; Cölfen, H.; Antonietti, M. *Inorg. Chim. Acta* **1998**, *280*, 348−354. Sidorov, S. N.; Bronstein, L. M.; Valetsky, P. M.; Hartmann, J.; Cölfen, H.; Schnablegger, H.; Antonietti, M. *J. Colloid Interface Sci.* **1999**, *212*, 197−211. Qi, L.; Cölfen, H.; Antonietti, M. *Nano Lett.* **2001**, *1*, 61−65. Bronstein, L. M.; Sidorov, S. N.; Valetsky, P. M.; Hartmann, J.; Cölfen, H.; Antonietti, M. *Langmuir* **1999**, *15*, 6256−6262. Sidorov, S. N.; Bronstein, L. M.; Kabachii, Y. A.; Valetsky, P. M.; Soo, P. L.; Maysinger, D.; Eisenberg, A. *Langmuir* **2004**, *20*, 3543−3550.

(4) de Laat, A. W. M.; Schoo, H. F. M. *J. Colloid Interface Sci.* **1997**, *191*, 416−423. de Laat, A. W. M.; Schoo, H. F. M. *J. Colloid Interface Sci.* **1998**, *200*, 228−234. de Laat, A. W. M.; Bijsterbosch, H. D.; Cohen Stuart, M. A.; Fleer, G. J.; Struijk, C. W. *Colloids Surf., A* **2000**, *166*, 79−89. Hoogeveen, N. G.; Cohen Stuart, M. A.; Fleer, G. J. *Colloids Surf., A* **1996**, *117*, 77−88. Yu, S.-H.; Cölfen, H.; Fischer, A. *Colloids Surf., A* **2004**, *243*, 49−52.

(5) Marentette, J. M.; Norwig, J.; Stockelmann, E.; Meyer, W. H.; Wegner, G. *Adv. Mater.* **1997**, *9*, 647−651. Sedlak, M.; Antonietti, M.; Cölfen, H. *Macromol. Chem. Phys.* **1998**, *199*, 247−254. Cölfen, H.; Antonietti, M. *Langmuir* **1998**, *14*, 582−589. Cölfen, H.; Qi, L. *Chem.—Eur. J.* **2001**, *7*, 106−116. Yu, S.-H.; Cölfen, H.; Hartmann, J.; Antonietti, M. *Adv. Funct. Mater.* **2002**, *12*, 541−545. Endo, H.; Schwahn, D.; Cölfen, H. *J. Chem. Phys.* **2004**, *120*, 9410−9423. Rudloff, J.; Antonietti, M.; Cölfen, H.; Pretula, J.; Kaluzynski, K.; Penczek, S. *Macromol. Chem. Phys.* **2002**, *203*, 627−635. Rudloff, J.; Cölfen, H. *Langmuir* **2004**, *20*, 991−996. Chen, S.-F.; Yu, S.-H.; Wang, T.-X.; Jiang, J.; Cölfen, H.; Hu, B.; Yu, B. *Adv. Mater.* **2005**, *17*, 1461−1465.

(6) Qi, L.; Cölfen, H.; Antonietti, M. *Angew. Chem., Int. Ed.* **2000**, *39*, 604−607. Qi, L.; Cölfen, H.; Antonietti, M. *Chem. Mater.* **2000**, *12*, 2392−2403. Robinson, K. L.; Weaver, J. V. M; Armes, S. P.; Diaz Marti, E.; Meldrum, F. C. *J. Mater. Chem.* **2002**, No. 12, 890−896. Li, M.; Cölfen, H.; Mann, S. *J. Mater. Chem.* **2004**, *14*, 2269−2276. Guillemet, B.; Faatz, M.; Groehn, F.; Wegner, G.; Gnanou, Y. *Langmuir* **2006**, *22*, 1875−1879.

(7) Taubert, A.; Palms, D.; Weiss, O.; Piccini, M.-T.; Batchelder, D. N. *Chem. Mater.* **2002**, *14*, 2594−2601. Taubert, A.; Glasser, G.; Palms, D. *Langmuir* **2002**, *18*, 4488−4494. Taubert, A.; Kübel, C.; Martin, D. C. *J. Phys. Chem. B* **2003**, *107*, 2660−2666.

(8) Gérardin, C.; Buissette, V.; Gaudemet, F.; Anthony, O.; Sanson, N.; DiRenzo, F.; Fajula, F. *Mater. Res. Soc. Symp. Proc.* **2002**, *726*, 249. Bouyer, F.; Sanson, N.; Destarac, M.; Gerardin, C. *New J. Chem.* **2006**, *30*, 399−408.

(9) Gérardin, C.; Sanson, N.; Bouyer, F.; Fajula, F.; Putaux, J.-L.; Joanicot, M.; Chopin, T. *Angew. Chem., Int. Ed.* **2003**, *42*, 3681−3685.

(10) Baccile, N.; Reboul, J.; Blanc, B.; Coq, B.; Lacroix-Demazes, P.; In, M.; Gérardin, C. *Angew. Chem., Int. Ed.* **2008**, *47*, 8433−8437. Warnant, J.; Reboul, J.; Aqil, A.; Cacciaguerra, T.; Jerome, C.; Gerardin, C. *Powder Technol.* **2011**, *208*, 461−466.

(11) Cölfen, H.; Antonietti, M. *Angew. Chem., Int. Ed.* **2005**, *44*, 5576−5591.

(12) Xu, A.-W.; Ma, Y.; Cölfen, H. *J. Mater. Chem.* **2007**, *17*, 415−449. Yu, S.-H.; Cölfen, H. *Macromol. Eng.* **2007**, *4*, 2597−2643.

(13) Riess, G. *Prog. Polym. Sci.* **2003**, *28*, 1107−1170. Cölfen, H. *Macromol. Rapid Commun.* **2001**, *22*, 219−252.

(14) Cohen Stuart, M. A.; Hofs, B.; Voets, I. K.; De Keizer, A. *Curr. Opin. Colloid Interface Sci.* **2005**, *10*, 30−36. Voets, I. K.; De Keizer, A.; Cohen Stuart, M. A. *Adv. Colloid Interface Sci.* **2009**, *147−148*, 300−318.

(15) Kataoka, K.; Kwon, G. S.; Yokoyama, M.; Okano, T.; Yasuhisa, S. *J. Controlled Release* **1993**, *24*, 119−132. Harada, A.; Kataoka, K. *Macromolecules* **1995**, *28*, 5294−5299.

(16) Kabanov, A. V.; Bronich, T. K.; Kabanov, V. A.; Yu, K.; Eisenberg, A. *Macromolecules* **1996**, *29*, 6797−6802.

(17) Cohen Stuart, M. A.; Besseling, N. A. M.; Fokkink, R. G. *Langmuir* **1998**, *14*, 6846−6849. Van der Burgh, S.; de Keizer, A.; Cohen Stuart, M. A. *Langmuir* **2004**, *20*, 1073−1084.

(18) Gohy, J.-F.; Varshney, S. K.; Antoun, S.; Jerome, R. *Macromolecules* **2000**, *33*, 9298−9305. Kakizawa, Y.; Harada, A.; Kataoka, K. *J. Am. Chem. Soc.* **1999**, *121*, 11247−11248. Reboul, J; Nugay, T.; Anik, N.; Cottet, H.; Ponsinet, V.; In, M.; Lacroix-Desmazes, P.; Gérardin, C. *Soft Matter* **2011**, *7*, 5836−5846.

(19) Bronich, T. K.; Kabanov, A. V.; Kabanov, V. A.; Yu, K.; Eisenberg, A. *Macromolecules* **1997**, *30*, 3519−3525. Kabanov, A. V.; Bronich, T. K.; Kabanov, V. A.; Yu, K.; Eisenberg, A. *J. Am. Chem. Soc.* **1998**, *120*, 9941−9942. Li, Y.; Nakashima, K. *Langmuir* **2003**, *19*, 548−553. Berret, J.-F.; Vigolo, B.; Eng, R.; Herve, P.; Grillo, I.; Yang, L. *Macromolecules* **2004**, *37*, 4922−4930.

(20) Katayose, S.; Kataoka, K. *J. Pharm. Sci.* **1998**, *87*, 160−163. Oupicky, D.; Konak, C.; Ulbrich, K.; Wolfert, M. A.; Seymour, L. W. *J. Controlled Release* **2000**, *65*, 149−171. Oupicky, D.; Konak, C.; Ulbrich, K. *Mater. Sci. Eng.* **1999**, *7*, 59−65.

(21) Li, Y.; Gong, Y.-K.; Nakashima, K.; Murata, Y. *Langmuir* **2002**, *18*, 6727−6729. Wu, K.; Shi, L.; Zhang, W.; An, Y.; Zhu, X.-X.; Zhang, X.; Li, Z. *Soft Matter* **2005**, *1*, 455−459. Bronich, T. K.; Keifer, P. A.; Shlyakhtenko, L. S.; Kabanov, A. V. *J. Am. Chem. Soc.* **2005**, *127*, 8236−8237.

(22) Bouyer, F.; Gérardin, C.; Fajula, F.; Putaux, J.-L.; Chopin, T. *Colloids Surf., A* **2003**, *217*, 179−184.

(23) Sanson, N.; Bouyer, F.; Gérardin, C.; In, M. *Phys. Chem. Chem. Phys.* **2004**, *6*, 1463−1466.

(24) Sanson, N.; Putaux, J.-L.; Destarac, M.; Gérardin, C.; Fajula, F. *Macromol. Symp.* **2005**, *226*, 279−288.

(25) Allouche, L.; Gérardin, C.; Loiseau, T.; Ferey, G.; Taulelle, F. *Angew. Chem., Int. Ed.* **2000**, *39*, 511−514.

(26) Taton, D.; Destarac, M.; Zard, S. Z., Macromolecular Design by Interchange of Xanthates: Background, Design, Scope and Applications. In *Handbook of RAFT Polymerization*; Barner-Kowollik, C, Ed.; Wiley-VCH: Weinheim, 2008; Chapter 10, p 373.

(27) Taton, D.; Wilczewska, A.-Z.; Destarac, M. *Macromol. Rapid Commun.* **2001**, *22*, 1497−1503.

(28) Sears, V. F. *Neutron News* **1992**, *3*, 26−37.

(29) Endo, N.; Shirota, H.; Horie, K. *Macromol. Rapid Commun.* **2001**, *22*, 593−597. Staikos, G.; Bokias, G.; Karayanni, K. *Polym. Int.* **1996**, *41*, 345−350. Mun, G. A.; Nurkeeva, Z. S.; Khutoryanskiy, V. V.; Sarybayeva, G. S.; Dubolazov, A. V. *Eur. Polym. J.* **2003**, *39*, 1687−1691. Mun, G. A.; Khutoryanskiy, V. V.; Akhmetkalieva, G. T.; Shmakov, S. N.; Dubolazov, A. V.; Nurkeeva, Z. S.; Park, K. *Colloid Polym. Sci.* **2004**, *283*, 174−181.

(30) de Gennes, P. G. *Scaling Concepts in Polymer Physics*; Cornell University Press: Ithaca, NY, 1979.

(31) Sabbagh, I.; Delsanti, M. *Eur. Phys. J. E: Soft Matter Biol. Phys.* **2000**, *1*, 75−86. Heitz, C.; Francois, J. *Polymer* **1999**, *40*, 3331−3344. Axelos, M. A. V.; Mestdagh, M. M.; Francois, J. *Macromolecules* **1994**, *27*, 6594−6602. Volk, N.; Vollmer, D.; Schmidt, M.; Oppermann, W.; Huber, K. In *Polyelectrolytes with Defined Molecular Architecture II*; Schmidt, M., Ed.; Springer: Berlin, 2004; p 29. Sabbagh, I.; Delsanti, M.; Lesieur, P. *Eur. Phys. J. B* **1999**, *12*, 253−260. Francois, J.; Heitz, C.; Mestdagh, M. M. *Polymer* **1997**, *38*, 5321−5332.

(32) Pedersen, J. S.; Gerstenberg, M. C. *Macromolecules* **1996**, *29*, 1363−1365.

(33) Pedersen, J. S. *J. Appl. Crystallogr.* **2000**, *33*, 637−640. Pedersen, J. S. *J. Chem. Phys.* **2001**, *114*, 2839−2846. Pedersen, J. S.; Svaneborg, C. *Curr. Opin. Colloid Interface Sci.* **2002**, *7*, 158−166.

(34) Antonietti, M.; Bremser, W.; Schmidt, M. *Macromolecules* **1990**, *23*, 3796−3805. Qin, A.; Tian, M.; Ramireddy, C.; Webber, S. E.; Munk, P. *Macromolecules* **1994**, *27*, 120−126. Hirzinger, B.; Helmstedt, M.; Stejskal, J. *Polymer* **2000**, *41*, 2883−2891.
(35) Lee, A. S.; Bütün, V.; Vamvakaki, M.; Armes, S. P.; Pople, J. A.; Gast, A. P. *Macromolecules* **2002**, *35*, 8540−8551. Förster, S.; Hermsdorf, N.; Boettcher, C.; Lindner, P. *Macromolecules* **2002**, *35*, 4096−4105. Pispas, S.; Hadjichristidis, N. *Langmuir* **2003**, *19*, 48−54.
(36) Hamley, I. W. *The Physics of Block Copolymers*; Oxford Science Publication: Oxford, U.K., 1998. Alexandridis, P.; Lindman, B. *Amphiphilic Block Copolymers*; Elsevier Science: New York, 2000.